Edaphic and geomorphic evidences of water level fluctuations in Gallocanta Lake, NE Spain

C. Castañeda[1*], F. Javier Gracia[2], E. Luna[1], R. Rodríguez-Ochoa[3]

[1]*Estación Experimental de Aula Dei, CSIC, Av. Montañana 1005, 50059 Zaragoza, Spain*

[2]*Departamento de Ciencias de la Tierra, Universidad de Cádiz, 11510 Puerto Real-Cádiz, Spain*

[3]*Departamento de Medio Ambiente y Ciencias del Suelo, Universitat de Lleida, Av. Rovira Roure 191, 25198 Lleida, Spain*

*Corresponding author: Carmen Castañeda; ccastaneda@eead.csic.es; Phone: +34 976 716069; Fax: +34 976 716145.

Abstract

The pedological implications of lake water level fluctuations are complex, especially in lake margin, where topographical, hydrological, and sedimentary conditions are most variable. Lake water level fluctuations generate landscape elements, which provide insights into the processes involved in soil development and the extent of the zones affected by flooding/desiccation. Coupling information from detailed geomorphological inspections in the field, the mapping of the lakeshore, and the pedogenesis of each landscape element can provide a better understanding of these relationships, which was used to study the saline Gallocanta Lake, NE Spain, a semiarid intramontane lacustrine system that undergoes significant and rapid water level fluctuations. Geomorphic classification of the lake margin forms and environments served as a guide for soil sampling. The geomorphological survey revealed high diversity and contrast in the lake margin environment, from shores affected by coastal erosion to zones characterized by progradation/aggradation. Two soil toposequences and 11 pedons that were on different geomorphic units were studied on two margins of the lake. Following gradients in elevation, moisture, and salinity, soils showed a succession of Inceptisols to Aridisols, with Mollisols developed at intermediate positions and Aquic soils at the lake floor and southern shore. Soils had a sandy, loamy texture and a predominantly carbonatic composition, high variation in CCE (mean =37%), texture, and coarse fragments throughout the soil profiles. Soil salinity was highest at the lowest topographic position and in the upper soil horizons, where mean ECe = 188.6 dS m^{-1} at 25 ºC. In addition, the highest organic matter (6%) and gypsum (34%) content occurred at the lake floor. Soil color characteristics and concentrations, and depletions of Fe and Mn indicated redox changes associated with soil water saturation under carbonate and or saline conditions. Macro and micromorphological features of oxidized and reduced horizons indicated the alternation between palustrine (reduced) and non-palustrine (detrital, emerged, oxidized) events at different geomorphic and topographic positions, from the lake floor up to 7 m above it. Pedogenesis inferred and the littoral/submerged forms located at permanently emerged areas confirmed the past and present trend toward the desiccation of the lake. This study has improved our understanding of how soils form and develop within the context of geomorphic units, and can be used in making land-use decisions in the protected reserve and agricultural surroundings of the lake.

Key words: *Holocene; lacustrine; playa-lake; saline; soil salinity; wetlands;*

1. Introduction

In recent decades, recognition of the benefits of wetlands has increased. In particular, saline wetlands provide important habitats for biodiversity conservation; however, a lack of information has hampered the conservation of many saline wetlands, which suffer the effects of high human pressure due to intensive agricultural and urban developments. Protected areas are essential for the conservation of the habitats needed to support plants, animals, and extremophiles. Wetland protection requires previous delimitation and the delineation of thematic maps that identify the connections between landscape features, hydrology, soils, and vegetation.

Unlike large inland and coastal saline lakes, which usually have particular hydrological conditions (Plotnikov and Aladin, 2011), most medium- and small-sized saline lakes are shallow, particularly, if precipitation is strongly seasonal, such as it is in the Mediterranean region and other arid and semi-arid zones (Beklioglu et al., 2007). Frequent and substantial fluctuations in water levels are a common characteristic of most shallow saline lakes; however, few studies have examined the relationships between lake water level fluctuations and the soils of inland saline wetlands. Soil moisture, flooding regime, and soil salinity have the most influence on the conditions in those wetlands. Soil processes are influenced by wetland hydrology, and some soil features can indicate specific environmental conditions.

Wetlands that have saline, hydromorphic soils are especially suited to the study of the processes that dictate the development of ecosystems. Redoximorphic features in a soil profile (Vepraskas, 1994; Otero and Macías, 2001; Richardson and Vepraskas, 2001) are indicators of hydric soils, and have been used to identify wetlands (Brower and Fitzpatrick, 2002; Hurt and Vasilas, 2006; Johnson et al., 2011).

In addition, few studies have investigated the geomorphology of saline lakes. Although many classic studies examined the nature and typology of patterned ground and polygonal cracking on dried lacustrine bottoms (Vinogradov, 1955; Hunt and Washburn, 1966; Neal, 1972), few studies have examined the morphosedimentary characteristics of saline lake margins and the effects of fluctuations in lake water levels (Evans et al., 1964; Eugster and Hardie, 1978; Isla and Bassani, 1992, Blair, 1999).

Lake water level fluctuations during the Quaternary have received much attention, mainly because they can be used to identify past climatic and environmental changes. Usually, the fluctuations are identified by interpreting the paleoecological (e.g., diatoms, ostracods, pollen) (Gouramanis et al., 2010; Hoffmann et al., 2012) or sedimentological proxies (De Cort et al., 2013) in drill cores. In other cases, lacustrine terraces have been studied for this purpose (Bowman, 1971; Flower and Foster, 1992; Gracia, 1995; Komatsu et al., 2010; Ocakoglu et al., 2013). Most of the studies of recent changes in lake water levels have focused on the effects of climatic and hydrological changes (Comín et al., 1991; Mason et al., 1994; Rodó et al., 2002) or the effects of human activities on sediments and the environment (Ahn et al., 2006; Merlín-Uribe et al., 2011). Few studies have reconstructed recent morphological changes of saline shallow lakes, most of which were in Africa (Ghienne et al., 2002; Drake and Bristow, 2006; Burrough and Thomas, 2009). In those studies, the hydric changes in shallow lakes had a strong influence on shoreline soils. Thus, the study of shoreline soils can provide insights into historical fluctuations in the water levels of saline lakes. Few studies of semi-arid and shallow saline lakes have integrated pedological processes and geomorphologic features at a detailed scale. The objective of this study is to identify the relationships between the pedological characteristics and the geomorphic processes at

Gallocanta Lake Basin, NE Spain, and their capacity to indicate past geomorphic processes and water level fluctuations in the lake.

2. Study area

2.1 Geographical and geological setting

Gallocanta Lake (40.98º N -1.51º E), the largest and most undisturbed saline lake in Western Europe, is located in a Quaternary Depression (about 543 km^2) within the Iberian Range (NE Spain), at 1000 m a.s.l. (Fig. 1). The 14.43-km^2 lake is 7.8 km long in the NW-SE direction and 2.8 km wide. The lacustrine basin is elongated in the NW-SE direction in parallel with the mountain range that borders the NE side of the basin, which has peaks up to 1400 m a.s.l. The NE mountain range is constituted by Ordovician silica-rich rocks; e.g., quartzites and slates, and it flanks to the South an extensive fault-bounded outcrop of deformed Mesozoic, mainly carbonatic, units (limestones and marls, Fig. 1). The lake is on impermeable Upper Triassic materials (lutites and interbedded evaporites), which contributes to the high salinity of the lake, which is highest in summer, when the water level is lowest. Groundwater salinity ranges between 0.5 and 49.4 dS m^{-1} (García-Vera et al., 2009).

The climate in the zone is dry, semi-arid mesothermic (Liso and Ascaso, 1969). Between 1944 and 2012, mean annual rainfall was 487 mm (range = 761 mm in 1959 to 232 mm in 2001) at Tornos weather station (Fig. 1). Rainfall in the area is irregular and, at least between 2000 and 2012, mean annual rainfall was 22% lower at the lakeshore (Los Picos weather station) (Fig. 1) than it was at Tornos weather station. May (mean = 73 mm) and July (mean = 27 mm) usually are the wettest and the driest months, respectively. Between 1944 and 2012, the mean annual temperature was 11.3 ºC, with

25% frost days per year. Maximum extreme temperatures occurred in 2001 (-22 °C) and 2012 (38.2 °C). Between 2000 and 2005, the mean annual hydric deficit was 605 mm, with evaporation of the lake >1000 mm year^{-1} (García-Vera and Martínez-Cob, 2004). The frequent NW and W winter winds, which reach speeds of >80 km h^{-1}, and the NE summer winds exacerbate the hydric deficit (Martínez-Cob et al., 2010). Those strong prevailing winds generate waves and currents in the lake, which usually propagate toward the SE (Gracia, 2014).

Soil temperature regime is mesic, and the soil moisture regime is xeric in agricultural areas and aquic (Soil Survey Staff, 2014) at the lakeshore. Between 2000 and 2005, mean temperature 6 cm below the soil surface was 13.4 ºC at the lake shoreline (García-Vera and Martínez-Cob, 2004).

Figure 1

A 6477-ha Natural Reserve encompasses the lake, the fringes of natural vegetation that cover the lake margins, and the peripheral agricultural lands. The area is protected under EU Birds and Habitats Directives and included in the Ramsar list (Ramsar Convention Secretariat, 2010). Most of the area is devoted to rainfed agriculture, winter cereals (mainly rye) and, occasionally, sunflower. To mitigate the reduction in the water level of the lake that has occurred recently (Fig. 2, García-Vera et al., 2009), irrigation from pumping wells has been reduced. Alternating wet (flooding) and dry (drought) periods, and the variation in salinity have led to the formation of biological communities that contain species that are adapted to droughts (Gómez et al., 1981). The vegetation in the SW margin includes prairies of *Salicornia patula*, *Puccinellia pungens,* and *Limonium costae* near the lakeshore, and prairies of *Juncus* and *Bolboschoenus maritimus* closer to the crops. In the NE margin, the most saline fringe of vegetation includes *Aeluropus* *littoralis*, *Suaeda splendens*, *Suaeda spicata*, *Salicornia patula*, *Sphenopus divaricatus,* and *Limonium costae*. Plants such as *Elymus* cf. *pungens*, *Dactylis glomerata*, *Medicago sativa*, *Tragopogon dubius,* and *Crepis pulchra* occur in uncultivated agricultural plots.

The water in the lake is vital for the biodiversity of the area, especially, for the well being of thousands of migratory and wintering birds (Leranoz and González, 2009). The amount of water the lake holds changes naturally at various time-scales (Comín et al., 1991; Rodó et al., 2002; Díaz de Arcaya et al., 2005; Luzón et al., 2007a; Castañeda and Herrero, 2009; García-Vera et al., 2009; Gracia, 2009). Since 1974 (Fig. 2) there have been several drought periods in which the water level of the lake was at or near zero, and a very wet period in the mid-1970s, with a maximum registered water level of 2.8 m in 1974 (Pérez, 2014).

Figure 2

2.2 Geomorphological setting

Various levels of stepped Quaternary alluvial fans and pediments develop on both margins of the Gallocanta depression. Most of the NE side of the lacustrine basin has a steep slope, influenced by its proximity to the mountain range, where the peaks are about 400 m above the lake floor. The SW side has a gentle relief, which is the result of carbonate outcrops that have been affected by intense karstic weathering and relief lowering, which have peaks that are < 50 m above the lake floor (Fig. 3).

The depression is a karst polje that developed during the Quaternary (Gracia et al., 2002). Several weathering planation surfaces occur in the basin, and the lowest two surround the main lake on the S, SW, and W sides, which develop on Jurassic limestones. The depression and the planation surfaces probably formed after a regional extensional tectonic phase in the Late Pliocene (Gutiérrez et al., 2008). At that time, the lowering of the local water table, which would have promoted vertical dissolution (until the epiphreatic zone was reached), caused the deepening of the polje bottom and the development of stepped planation surfaces. Once the polje floor reached the impervious Triassic substratum, a stable lacustrine system developed. Consequently, the formation of Gallocanta Lake is associated with the interruption of the deepening of the polje about 12,200 yr BP, in the Late Pleistocene (Burjachs et al., 1996). Lacustrine sediments under the lakebed are only about 1-2 m thick; however, they reflect various climatic and environmental changes caused by flooding and desiccation (Schütt, 1998; Rodó et al., 2002). Calvo et al. (1978) analysed the mineralogy of the lake bottom sediments and their vertical variations in some cores made on the centre of the lake. Pérez et al. (2002) and Luzón et al. (2007a) studied the stratigraphical record and sedimentology of the lake bottom sediments through several cores made along a transect NE-SW oriented and used the data to interpret environmental and climatic changes during the Holocene.

In summary, the low plains surrounding the lake are formed by sedimentary flats, mostly covered by halophytes, while rock outcrops near the lake only appear on the western margin, where some planation surfaces on Jurassic carbonates extend to the lake (Fig. 1). Elsewhere, the lake is surrounded by a set of alluvial fans and lacustrine terraces that are elevated a few meters relative to the lake bottom.

3. Methods

Geomorphological photointerpretation and mapping, as well as systematic field inspection of the lake margins were improved with respect to previous studies (Castañeda et al., 2013). Airborne LIDAR data for the lake and surrounding areas were obtained from the National Geographic Institute, with an absolute vertical accuracy of

0.20 m and a density of 0.5 p × m^{-2}. The resulting topographic model was used for an accurate location and height definition at a sub-metric scale of the different landscape elements previously recognized along the lake margins. Soils were sampled at the two longest margins of the lake based on a geomorphological map of the central section of the lake (Castañeda et al., 2013). The sampling sites of the 11 soil profiles were along one of two toposequences (about 1500 m and 2000 m long) that crossed the northern and southern margins of the lake, respectively (Fig. 3). Both transects covered gradients in moisture and soil salinity. The profiles were dug within various geomorphic units, between the pediments and the lake floor, in parallel with the plant communities, from the crops to the halophyte fringes and the bare lake floor. The elevation of the sampling sites relative to the elevation of the lakebed ranged from 4.3 m at the southern margin to 15.3 m at the northern margin (Table 2).

Soil sampling was performed in October 2010, and in July and October 2011. In 2010 and 2011, the annual rainfall was 359 mm and 276 mm, or 74% and 54% of the mean annual rainfall (487 mm), respectively. At lake level (Los Picos weather station, Fig. 1), rainfall was very low in 2011 (156 mm). Pits that reached the water table had to be bailed out several times and an auger was used to collect soil samples. Fifty-two soil samples were collected and specific horizons were sampled for micromorphological analyses.

Soil samples were air-dried at room temperature before being dried in an oven at ≤ 40ºC, and sieved through a 2-mm mesh. Soil salinity was measured as the electrical conductivity of the 1:5 soil:water extract (EC1:5) and the saturated paste extract (ECe) (United States Salinity Laboratory Staff, 1954). Electrical conductivities were expressed in dS m^{-1} at 25ºC. Calcium carbonate equivalent (CCE) was quantified by gasometry, gypsum content was quantified by thermogravimetry (Artieda et al., 2006), and organic matter (OM) was quantified by chromic-acid digestion and spectrophotometry. Texture was assessed by laser diffraction, with a correction for the clay value (following Taubner et al., 2009). To compare the soil profiles, we calculated the proportions of CCE, gypsum, OM, sand, silt, and clay at soil depth intervals of 25 cm, and these layers were designated as 'synthetic layers 25 cm depth'. The values from the synthetic layers were the mean of the soil samples weighted by their depth interval (http://digital.csic.es/handle/10261/60892), up to 150 cm or to the maximum depth of the shallowest pits. Genetic and diagnostic horizons and soil taxonomic classifications were based on Soil Survey Staff (2014). Thin sections (135 × 58, and 58 × 42 mm large) of the horizons were prepared based on the method of Guilloré (1985), after they had been impregnated with a cold-setting polyester resin, and described following Stoops (2003).

Figure 3

4. Results

4.1 Geomorphological context of the two lake margins

The NE and the SW shores of the lake differ in several important respects. The structurally controlled morphological asymmetry of the depression makes the fans on the northern margin short (mean length = 1.5 km), with a mean slope of 4%. Those fans are about 6 m higher than the lake bottom, and mainly comprise quartzitic boulders and coarse gravels. Streams reaching the lake in this margin are ephemeral and inset on the fans forming flat-bottomed valleys filled with colluvial sediments (Fig. 4). In the valley bottoms, the high water table gives rise to springs and small wetlands near the lakeshore, where the longitudinal valley gradients are lower.

Inset on the fans, a 300-m wide plain has developed on a lacustrine terrace about 2 m higher than the lakebed (Figs. 4 and 5A), which is characterized by four small elongated vegetated marginal wetlands, marshes, and palustrine zones broadly parallel to the main lakeshore. Those located on the east side of the lake receive water from a valley coming from the mountain range, which has caused the wetlands to expand. Each wetland has a central wet area fringed by marshes or crops mostly elongated parallel to the lakeshore. The wetlands are separated from the lake by a narrow sandy barrier covered with pioneering halophytes (*Salicornia*) (Fig. 5B) or by a narrow beach (about 0.5 m high) fringed by hygrophilous vegetation (*Juncus*) (Fig. 5C). A continuous low cliff < 1 m high affects the sedimentary units along this NE lake margin. The concentration of wave energy caused by the orientation of the lake and the prevailing winds contribute to the eroded nature of this shoreline.

Figure 4

Figure 5

The southern fans that reach the lake are large (> 8 km long), have a gentle (mean < 1%) slope, and comprise medium-sized polymictic gravels to sands. Most of those fans originate at the foot of low reliefs and outcrops of Jurassic and Cretaceous limestones. The largest fan, which is closest to the lake, is about 10 m above the lakebed. The main fluvial water and sedimentary input to the lake (Los Pozuelos Arroyo, Fig. 3) is at a central point on the SW shore, which leads to a small delta. An abandoned paleovalley associated with this arroyo can be recognized to the west of the present, active mouth. This arroyo is an ephemeral channel (Fig. 7A) that drains a > 100-km^2 basin which represents the most important source of sediment supply to Gallocanta Lake. Consequently, the SW margin has a predominantly sedimentary character, forming a wide (up to > 600 m) planar fringe, inset >5 m on the lowest karstic planation surface of the basin.

The SW lake shore is formed by a series of parallel bands, mostly vegetated, where vegetation density increases with elevation. Connections between adjacent plains consist of small declines and degraded low cliffs. At about 1 m above the lake floor, a wide sedimentary active zone has formed, comprising several sandy barrier islands and sublittoral bars, most of which are roughly parallel to the shore, 150-500 m long, 50-100 m wide, usually < 1 m high, and proceed to the lake over gentle declines (Figs. 6 and 7B). Between the sandy barrier and the mainland, a usually dry lagoon develops, which is covered by bare muds. Wind-driven waves in the lake create a prevailing longshore current to the SE. Various sedimentary bodies and recurved spits, similar to those of marine coasts, develop parallel to this prevailing current. Differences in exposure to waves and currents have dictated the nature of the sedimentary forms and their prevailing texture: sands in the most exposed outer faces of the islands and bars, silts in the sheltered zones, and clays in the completely protected lagoon (Fig. 6). Progradation and progressive emergence of the SW lake shore is producing a shifting of the lake bottom to the NE. Sedimentary aggradation in the sheltered lagoon is indicated by the partial burial of vegetation remains and tumbleweeds that reach this zone and are apparent during droughts.

In addition to promoting erosion or sedimentation in the lake margins, past lake water level fluctuations have influenced the shifting of the border between natural vegetation and agricultural lands. In recent years, the water level of the lake has remained low (Fig.

2), and the area near the lake devoted to crops has expanded in parallel to the natural shaping and reworking of the shoreline landforms.

Figure 6

Figure 7

4.2 Soil composition and morphology

The depth of the studied pedons ranges from 60 cm at the highest landscape position, the alluvial fan, to 185 cm at the lake floor. Groundwater was reached in 9 out of the 11 profiles, even in soils > 6 m above the lake floor (GA25). Groundwater is saline (up to 114 dS m^{-1}) at the lake floor (GA28 and GA29), sublittoral sand bars (GA19, GA27), and the lagoon (GA20). Non-saline groundwater was reached at GA25 and GA 26 at the NE margin, and at GA21 and at GA22 at the SW margin (Table 1).

Table 1

Soil pH ranges from 7.6 to 8.7 (Table 2). ECe and EC1:5 are strongly linearly correlated (R^2 = 0.91). Mean ECe is 36.6 dS m^{-1} (range = 0.3 - 188.6 dS m^{-1}). A majority (53.8%) of the soil samples are very strongly saline (ECe > 16 dS m^{-1}). For comparison purposes, based on the average ECe in the upper 50 cm, the soils are moderately saline (ECe up to 6.3 dS m^{-1}) at the sublittoral bars and the lagoon grasslands (Table 2), and very strongly saline (ECe up to 31.8 dS m^{-1}) at the lake floor. All of the other soils are non-saline except the upper soil horizon of the inactive beach (ECe = 3.4 dS m^{-1}). In the soil profile, soil salinity decreases with depth (Fig. 8), which reflects evapoconcentration in the upper horizons, in agreement with the hydric deficit (> 380 mm) accumulated in the months before the field seasons. Four of the eight pedons out of the lake floor support halophylic vegetation (Table 1).

Figure 8

The average calcium carbonate equivalent (CCE) is 37.3% (range = 3.9 - 72.2), with significant differences ($p < 0.05$) between the NE and SW margins (32.3% and 42.8%, respectively). Typically, the upper horizons have lower CCE than the deeper horizons (Table 2, Fig. 11). Mean gypsum content is 5.1%, and the highest concentrations occur in the upper horizons of the lake floor, pedons GA28 (28.6%) and GA29 (33.7%). The organic matter content (mean 1.3%) ranges from 0.3% to 6.3%, and is highest at the lake floor (Ayzg). Away from the lakebed, the organic matter accumulated in A and Ap horizons rather than in Ag horizons (Table 2).

Soils have a predominantly sandy and loamy texture, with a mean sand content of 56.7% (range = 12.5% - 96.4%), more than twice the mean content of silt (21.7%) or clay (25.6%). Sand content is 38% higher in the upper horizons than it is farther below and, frequently, sand content is high at a depth of about 100 cm, which corresponds to horizons with low clay content (Table 2, Fig. 11). The soil samples from the NE and SW margins of the lake differ significantly ($p < 0.05$) in silt content (25.8% and 17.2%, respectively). Fine to coarse gravels of quartzites and shales predominated, with the highest proportion (about 50%) at the paleovalley (GA22) and the alluvial fan (GA24) soils.

Table 2

Two main horizon sequences are recognized, A-C and A-Bwk-C (Table 2, Fig. 9), with frequent wavy boundaries between horizons. The diagnostic horizons (Soil Survey Staff, 2014) are Ochric, Mollic, Petrocalcic, Calcic, Gypsic and Salic. Calcic horizons occur at both lake margins, although best developed in the northern alluvial fan soils, and there are multiple generations of recemented breccia and laminae (GA23, Fig. 9). A discontinuous Bkm horizon occur at the subsurface (~100 cm) of the inactive beach, GA21 (Fig. 6). Carbonate coatings and pendants are common at several landscape positions, soft powdery carbonates are present in the southern soils, and carbonate nodules are common in the northern soils (Fig. 9). Gypsic and Salic horizons occur to a depth of 100 cm at the lake floor, and Salic horizons occur at the margins of the lake (GA19, GA20, GA27). Mollic horizons are present in the flat-bottomed valley. Soil classifications (Table 1) indicate that soil types are distributed among the geomorphic units in a consistent manner (Fig. 11).

Stone lines are at the lake floor, i.e., a 4-cm-thick stone line of fine, rounded quartz gravels in GA29, and at the northern pediment (Fig. 9). Here, a sandy layer with coarse subrounded quartzitic gravels and cobbles is found in GA24, and subhorizontally oriented subangular tabular quartzitic stones are parallel to the slope in the marsh soil (GA26).

Figure 9

4.3 Soil color and redoximorphic features

Soil surface horizons at the lake floor display the strongest gley hues (7.5B and 10B) and the lowest chroma (Table 2), and samples in the hand had a ‘rotten eggs’ odor. All of the soil surface horizons sampled at the SW margin exhibit a strong gleying matrix, with hue color 2.5Y and chroma ≤ 2, which indicates that they formed under reduced conditions. At the NE margin, soil chroma is ≤ 2; specifically, in the soils at the lowest landscape positions: the sand bar (GA27), the marsh (GA26), and the valley (GA25). At the alluvial fans, both the chroma and the hue of soil surface horizons increases with elevation (Table 2).

Iron and/or manganese mottles are present in all of the soils examined (Fig. 9), except at the alluvial fan (GA23 and GA24). Mottles rich in iron and/or manganese oxides have a chroma that ranges from 4 to 8, are common in surface horizons, and mainly are associated with pores, coarse fragments, and root channels. In subsurface horizons, these mottles are under either oxidizing or reducing conditions (i.e., GA19, GA20, GA28, and GA29 in the reducing matrix, and GA22, GA25, GA26, GA27 in the oxidizing matrix). Occasionally, the mottles form bands which reflect the circulation of water or air through preferential planes (GA29). In general, mottles poor in iron and/or manganese oxides have a chroma ≤ 2 and occur in horizons that are currently under reducing conditions.

Current reducing conditions are identified in soils at the lake floor (GA28 and GA29), the sublittoral sand bar (GA19), and the lagoon (GA20). Typically, gleying is strongest (chroma < 2) in the subsurface horizons of those soils. Other soil surface horizons with chroma ≤ 2 (GA21, GA22, GA25, GA26, GA27) are under oxidizing conditions, as indicated by their agro-pastoral use (e.g., GA22), which indicates that the (former) water saturation milieu that was responsible for the reducing conditions is no longer present. Nevertheless, all of the studied soils, except those at GA25 (Fig. 4), maintain the reduction in their subsurface horizons.

Micromorphological observations of the samples from surface horizons indicate a typical peloidal morphology (Platt, 1989; Freytet and Verrechia, 2002) of the micromass (Figs. 10A), with isolated or coalescent peds, and a blocky structure in the subsurface horizons (Fig. 10B). Lenticular gypsum is present as random crystal intergrowths (Fig. 10A). Carbonate coatings, some of which with sequential aggradation and dark rims, are common in the gravel-sized fragments of the Ap horizon (Fig. 10C), probably reworked by agricultural plowing. Some channels of the subsurface horizons exhibit a grey micritic coating (Fig. 10D), and carbonate recrystallization includes well developed crystals (Fig. 10E). Biological remains such as oogonia (Fig. 10F) and stems of *Charophyte*, shells of Ostracods (Fig 10G) and aquatic Gastropods, and phytolites are common in surface horizons. Other features associated with biological activity such as passage features with crescent internal fabric, chambers and channels, loose continuous and discontinuous microgranular infillings, are especially abundant in the subsurface horizons. Impregnative redoximorphic features such as Fe-Mn oxide hypocoatings with associated coatings (Fig. 10H) are present in aggregate faces along voids, which are reflected in the iron and or manganese mottles observed in the field.

Figure 10

5. Discussion

5.1 Soil composition and texture

The soils examined at Gallocanta Lake have a predominantly carbonatic composition (Table 2, Fig. 11). The significant differences in CCE between the northern and southern margins of the lake replicate the differences in the carbonate content of samples collected by Calvo et al. (1978) and agree with the observations of Aranzadi (1980). The highest carbonate content (e.g. CCE > 60%) occurs in soils of intermediate landscape positions (GA26, GA21, GA20 and GA19), probably because the persistently high, albeit fluctuating, water table favors the accumulation of pedogenic carbonates, including discontinuous cementations (GA21, Fig. 9). Following the increased expression of the carbonatic accumulation morphologies in arid environments (Schoeneberger et al., 2012), the petrocalcic horizon of the northern alluvial fan (GA23, Figs. 4 and 9) corresponds to the stage IV of pedogenic carbonate development. These oldest soils were described as caliche by Calvo et al. (1978) and as carbonate crust by Aranzadi (1980), and correspond to the IV development stage of Machette (1985). The common occurrence of non-cemented accumulations in the form of soft powdery carbonates or soft-to-indurated nodules (Fig. 9) provides evidence of present-day movements of carbonates throughout the landscape. Similar sequence of calcrete development in relation with palustrine environments in distal alluvial fans are described by AlShuaibi and Khalaf (2011) in Kuwait.

The variation in sedimentary processes and pedogenesis influenced the variation in CCE in the soil profile. The surface soil layers had the lowest CCE and clay content (Fig. 11, Table 2), in agreement with the observations of Calvo et al. (1978). Horizons with high CCE also have high clay content (Table 2), corresponding to prevailing lacustrine conditions.

In contrast to other saline wetlands in the Ebro Basin (Castañeda et al., 2013), at the Gallocanta basin the saline soils occur only at the lake floor and in neighboring narrow fringes where the groundwater is strongly saline (Table 1), or at sites with non-saline groundwater but subjected to occasional flooding; e.g., at the inactive beach (GA21). The salinity profiles of the two soils at the lake floor (GA28 and GA29) are similar and indicate a significant increase in salinity in the upper horizons (Fig. 8). Soils at the sand barriers and lagoon (GA19, GA20 and GA27) have intermediate salinity (Fig. 8), indicating a mixture of pluvial fresh and lacustrine saline groundwater at the lake margins.

The significant differences in the silt content of the two margins are indicated in the cores collected from a similar NE-SW transect by Pérez et al. (2002, in Fig. 8), who interpret the silt material as products of small deltaic systems, and Luzón et al. (2007a) indicate the outwashing from torrential flows as a source of the silt material. In the soil profile, the particle-size distribution expressed as synthetic values (Fig. 11) allows the identification of a sandy layer at a mean depth of 100 cm, consistently concordant with the topographic surface at the southern margin. Despite the shallow topographic gradient of this margin, the detrital supply from the Mesozoic outcrops reaches the lakebed with gradually attenuated energy, as sand content decreases from 94% at the margin to 68% at the lake floor. This alluvial material enters the lake probably favored by a low or near zero water level in the lake (i.e., a drought period), and it is not expressed in the soil profile of the sublittoral bar (GA19) because of its intense reworking by SW waves and longshore currents (Fig. 6). At the northern toposequence, sandy layers are also recognized (Fig. 11), and the shallowest sandy layer of GA27 soil indicates subsequent erosion of the bar due to the erosive character of this lake margin (Fig. 4). In addition to the textural changes (Table 2), the stone lines (Fig. 9) reveal pedogenic discontinuities (Ruhe, 1959) that are produced by erosional and/or depositional conditions (Brown et al., 2004; Splinter et al., 2005).

Figure 11

5.2 Soil hydric conditions along the toposequences

The toposequences at Gallocanta Lake demonstrate a strong correlation between geomorphology and soil distribution, with a progression of Inceptisols to Aridisols towards the lake, and Mollisols at intermediate positions. The periodic saturation experienced by some of the soils examined produces specific pedofeatures of aquic conditions (Vepraskas, 1994; Soil Survey Staff, 2014). The aquic soils (Gypsic Aquisalids) of the lake floor (GA28 and GA29) are submerged during high-water periods and emerged during low-water periods. They remain soaked with highly saline groundwater and are usually impassable (Table 1).

Aquic conditions and shallow groundwater prevail at the SW sublittoral sand bar, 0.4 m above the lake floor, with Typic Aquisalids (GA19).

Fringing the lake, soils are fed by water with half the salinity of the lake bottom (Table 1) and the aquic conditions do not persist. Typic Haplosalids are 2.2 m above the lake floor at the northern sand barrier (GA27) and 0.7 m above the lake floor at the lagoon (GA20). However, the Aquic Calcixerept (GA21) of the southern inactive beach (Fig. 6) indicates that aquic conditions reappear at the SW margin because of its low topographic gradient and the lateral supply of fresh groundwater (Table 2).

At the highest landscape positions (Fig. 11), under a xeric soil moisture regime, Typic (GA24) and Petrocalcic (GA23) Calcixerepts are in the northern alluvial fans whereas Pachic Calcixerolls develop in the valleys (Fig. 4), under former grassland (GA25) and marshes (GA26). The latest soils are favored by the fresh water seepage associated to the lateral groundwater flows from the mountain range, as indicated by the permanent raising of springs, the historical occurrence of non-saline prairies used for cattle grazing (L. XVII, Fig. 1 in Hernández-Pacheco and Aranegui, 1926), and the occasional waterlogging of the crops at the end of the valley.

Based on the criteria of Richardson and Vepraskas (2001), the soils at the lake floor (GA28 and GA29), the sandy bars and barriers (GA19 and GA27), the lagoon (GA20), and the inactive beach (GA21) are hydric soils.

5.3 Redoximorphic features and palustrine conditions

Information about redoximorphic processes in carbonate rich soils is scarce. Redoximorphic features can form in soils over several decades (Birkeland, 1999), although their expression can be limited in saline environments (Boettinger, 1977). In the saline and non-saline carbonate soils examined in this study, redoximorphic features are well expressed in the field and are consistent indicators of pedogenesis under subaqueous environment (Durand et al., 2010) and of oxidation and reduction conditions associated with rapid fluctuations of the water table (Lindbo et al., 2010).

Apart from redoximorphic features, other morphologic features of the studied soils, such as matrix color, carbonate content, whole-particle size distribution, and micromorphological pedofeatures (Fig. 10) indicate pedogenesis associated with palustrine conditions (reduced) according to the definition of Jackson (1997), and non-palustrine (detrital, emerged, oxidized) events (Fig. 9). On average, palustrine horizons have a small amount of (mean = 6%) coarse fragments, 48% sand content, and a clay/silt ratio of 1.7. In contrast, non-palustrine layers have high chroma (mean 4), high coarse fragments (mean 20%) and sand (mean 57%) content, and a mean clay/silt ratio of 2.2 (7.6 if the lowest GA29 horizon is included). In the soil profile, pedofeatures that reflect palustrine conditions usually occur from the soil surface to various depths (Fig. 9). The thickest soil subjected to palustrine conditions is more homogeneous at the NE margin (mean 125 cm) than it is at the SW margin (50 cm - 172 cm, Fig. 9).

Non-palustrine (detrital) layers occur systematically beneath the palustrine horizons, except at the lagoon (GA20), where palustrine and non-palustrine layers alternate (Fig. 9). The occurrence of palustrine and non-palustrine horizons in the soil profiles indicates a balance between clastic sedimentation supplied by arroyos that reach the lake during summer storms in dry periods, and lacustrine carbonatic deposition under humid conditions during high water level periods. This sequence differed from the one established for closed basins in dry climates (Boettinger and Richardson, 2001), with clastic sedimentation during humid periods and evaporite deposition under dry conditions.

5.4 Evidences of water level fluctuations

Hernández-Pacheco and Aranegui (1926) observed that the water level fluctuations of Gallocanta Lake translate into the retreating of the shoreline by 5 - 200 m, depending on the topography; however, the oldest available aerial photograph (Fig. 12A) taken during the wettest period since 1944, the 1970s (Luna et al., 2014), shows that the lake water invades the shorelines by > 700 m. The marshes at the northern margin are inundated, and the chain of islands at the southern margin is partially covered by water. In contrast, recent orthophotographs (Fig. 12B) show the lake margin emerged along with grey soils at elevations higher than the present-day lake floor. Those grey soils contrast with the reddish soils of the Ordovician materials and Quaternary alluvial fans. Grey soils must have originated due to the persistence of flooding and inundation patterns, common in palustrine environments, i.e., material growing or deposited in a marsh or marsh-like environment (Jackson, 1997).

The present-day hydrological regime of Gallocanta Lake is not compatible with soils subjected to intermittent flooding or waterlogging at high landscape positions; e.g., at 4.2 m (GA22) and 7 m (GA25) above the lake floor (Fig. 11). These soils are landscape indicators of the water level fluctuations and witnesses of the lake retreating during the Holocene. In previous studies, anoxic features are only mentioned at the lake floor (Luzón et al, 2007b). The evidence of palustrine conditions at positions several meters above the lake agrees with the water levels inferred from paleoclimatic and sedimentological data from core samplings (Comín et al., 1991; Pérez et al., 2002; Rodó et al., 2002; Luzón et al., 2007b).

Figure 12

The piezometric levels in the Gallocanta basin and the water levels recorded in the lake are strongly correlated (García-Vera et al., 2009), which is expected given the pluvial origin of the lake water. Thus, the fluctuations of groundwater level around the lake are expected to occur in concert with the fluctuations of the lake water level.

The soils at the lowest landscape positions around Gallocanta Lake are subjected to hydric variations associated with the present-day fluctuations in the lake water level. The upper layers of the soils in sandy barriers (GA19, GA27) exhibit submersion features (Fig. 9) which indicate flooding episodes after their formation as littoral sedimentary bodies. Erosion of the NE barrier island (Fig. 4) indicates a flooding episode that was long enough to generate strong littoral currents capable of eroding the lakeward side of this sedimentary structure. The progradation of the SW lake sandy shore and the sedimentary aggradation of the lagoon along the southern margin have promoted a progressive emergence of the southern shore and a decrease in the probability of a repetition of wetting/drying cycles in the future.

At the lake floor (Fig. 11), within the first 210 cm of the lake infill materials (Luzón et al., 2007a), pedological features are present to a depth of 90 cm. Similar to other environments where sediments are considered subaqueous soils (Demas and Rabenhorst, 1999), the sediments of Gallocanta Lake can been better understood if studies include an evaluation of soil processes.

Conclusions

Geomorphic and edaphic evidence of water level fluctuations were investigated in a shallow, strongly fluctuating, saline lake. Palustrine materials that had signals of past or present flood conditions indicated past hydric conditions that were correlated with lake water level fluctuations. The detailed analysis of the lake margin landscapes and forms provided insights into the prevailing types of processes: erosive, sedimentary-progradational, and sedimentary-aggradational.

The combination of geomorphological and pedological surveys improved the understanding of the soil formation processes and the geomorphological development of highly fluctuating lakeshores. The presence of landscape elements characteristic of littoral and submerged environments which are presently emerged, helped to explain the pedogenesis under palustrine conditions at high and non-flooded topographic positions.

The distribution of saline soils and the salinity gradients indicated the extent of the present-day lacustrine fringe that is subjected to intermittent flooding. In the soil profile, variations in carbonate content and particle-size distribution revealed pedogenic discontinuities that have been conditioned by sedimentological changes at the lake floor and in the surrounding area. The hydric soil indicators confirmed the present soil saturation at different topographic positions, in association with lateral subsurface water flows. Macro and micro soil characteristics (e.g., carbonatic, color spots and redoximorphic) indicated past palustrine conditions at different topographic and geomorphic positions, which were paralleled by the water level fluctuations of the lake during the Holocene and in historical times.

Relationships between soils and geomorphology were evident throughout the toposequences based on the redistribution of carbonate, gypsum, and salts, redoximorphic features, and the taxonomy of the soils. This study identified the early stages of pedogenesis at the lake floor, and that the most complex pedogenesis occurred in the lacustrine fringes that have been exposed to frequent fluctuations in water levels. The lake fringes had the most diverse and complex landscapes, and several inactive, residual forms confirmed the deductions made from the analysis of palustrine soils associated with them. In general, pedogenesis and geomorphology both reflect the trend of Gallocanta Lake towards more prolonged desiccation.

The pedofeatures examined can be used to identify hydric soils, current and past wetland soils, and to understand the pedogenic processes of lacustrine materials in relation to past and present geomorphological processes acting on them. The combination of edaphic and geomorphic investigations in other types of lakes (e.g., non-saline, permanent.) or to other types of lacustrine littoral environments (inlets, open wetlands, dunes) will provide valuable information for a better understanding of these complex environments.

Acknowledgements

This article is a result of the research project AGL2012-40100 funded by MINECO and is a contribution to Andalusian Research Group P.A.I. RNM-328. We acknowledge the data provided by the Spanish Meteorological Agency (AEMET). E. Luna was financed by a fellowship from the Government of Aragón, Spain. The 2006 orthoimages and LIDAR data were supplied by the National Geographic Institute of Spain (Instituto Geográfico Nacional).

References

Ahn, Y.S., Mizugaki, S., Nakamura, F., 2006. Historical change in lake sedimentation in Lake Takkobu, Kushiro Mire, northern Japan over the last 300 years. Geomorphology 78 (3-4), 321-334.

AlShuaibi, A.A., Khalaf, F.I., 2011. Development and lithogenesis of the palustrine and calcrete deposits of the Dibdibba Alluvial Fan, Kuwait. Journal of Asian Earth Sciences 42, 423-439.

Aranzadi, E., 1980. Estudios de impactos ambientales sobre la laguna de Gallocanta por la acción del desarrollo agrario. Consultant: Proyex S.A., Zaragoza. 184 pp. + maps.

Artieda, O., Herrero, J., Drohan, P.J., 2006. A refinement of the differential water loss method for gypsum determination in soils. Soil Sci. Soc. Am. J. 70, 1932-1935.

Beklioglu, M., Romo, S., Kagalou, I.; Quintana, X., Bécares, E., 2007. State of the art in the functioning of shallow Mediterranean lakes. Hydrobiologia 584, 317-326.

Birkeland, P.W., 1999. Soils and Geomorphology, 3rd edition. Oxford University Press, New York. 430 pp.

Blair, T.C., 1999. Sedimentology of gravelly Lake Lahontan highstand shoreline deposits, Churchill Butte, Nevada, USA. Sedimentary Geology 123, 199-218.

Boettinger, J.L., 1977. Aquisalids (Salorthids) and other wet saline and alkaline soils: problems identifying aquic conditions and hydric soils, pp 79-98, In M.J. Vepraskas and S.W. Sprecher: Aquic conditions and hydric soils: the problem soils. SSSA Special Publication No. 50, Wisconsin.

Boettinger, J.L., Richardson, J.L., 2001 Saline and wet soils of wetlands in dry climates, In J.L. Richardson and M.J. Vepraskas (eds.), Wetlands Soils: genesis, hydrology, landscapes and classification. CRC Press, Florida, US, pp. 383-390.

Bowman, D., 1971. Geomorphology of the shore terraces of the Late Pleistocene Lisan Lake (Israel). Palaeogeography, Palaeoclimatology, Palaeoecology 9, 183-209.

Brower, J., Fitzpatrick, R.W., 2002. Restricting layers, flow paths and correlation between duration of soil saturation and soil morphological features along a hillslope with an altered soil water regime in western Victoria. Australian Journal of Soil Research 40(6), 927-946.

Brown, D.J., McSweeney, K., Helme, P.A., 2004. Statistical, geochemical, and morphological analyses of stone line formation in Uganda. Geomorphology 62, 217–237.

Burjachs, F., Rodó, X., Comín, F.A., 1996. Gallocanta: ejemplo de secuencia palinológica en una laguna efímera. In: Ruiz Zapata, B. (ed.), Estudios Palinológicos. University of Alcalá, Alcalá de Henares, Spain, pp. 25-29.

Burrough, S.L., Thomas, D.S.G., 2009. Geomorphological contributions to palaeolimnology on the African continent. Geomorphology 103, 285-298.

Calvo, J., González, J.M., González, J., Villena, J., 1978. Primeros datos sobre la sedimentación de dolomía en la laguna de Gallocanta (provincias de Zaragoza y Teruel). Tecniterrae 21, 6-15.

Castañeda, C., Herrero, J. 2009. Application of Landsat and ERS imagery to the study of saline wetlands in semi-arid agricultural areas of NE Spain. Pp. 175-197. In Metternicht and Zinck (eds), Remote Sensing of Soil Salinization: Impact and Land Management. CRC Press, Boca Raton, FL. ISBN: 978-1-4200-6502-2.

Castañeda, C, Gracia, F.J., Meyer, A., Romeo, R., 2013. Coastal landforms and environments in the central sector of Gallocanta saline lake (Iberian Range, Spain). Journal of Maps 9(4), 584-589.

Comín F.A., Julià, R., Comín, P., 1991. Fluctuations, the key aspect ecological interpretation of ecosystems. Oecologia Aquatica 10, 127-135.

De Cort, G., Bessems, I., Keppens, E., Mees, F., Cumming, B., Verschuren, D., 2013. Late-Holocene and recent hydroclimatic variability in the central Kenya Rift Valley: The sediment record of hypersaline lakes Bogoria, Nakuru and Elementeita. Palaeogeography, Palaeoclimatology, Palaeoecology 388, 69-80.

Demas, G.P., Rabenhorst, M.C., 1999. Subaqueous Soils: Pedogenesis in a Submersed Environment. Soil Sci. Soc. Am. J. 63, 1250-1257.

Díaz de Arcaya, N., Castañeda C., Herrero J., Losada J.A., 2005. Cartografía de coberturas asociadas a las fluctuaciones de la Laguna de Gallocanta. Revista de la Asociación Española de Teledetección 24, 61-65.

Drake, N., Bristow, C., 2006. Shorelines in the Sahara: geomorphological evidence for an enhanced monsoon from palaeolake Megachad. Holocene 16, 901-911.

Durand, N., Monger, H.C., Canti, M.G., 2010. Calcium Carbonate Features. In: G. Stoops, V. Marcelino, and F. Mees (eds), Micromorphological features of Soils and Regoliths, Elsevier. pp. 149-194.

Evans, D.G., Kendall, C.G.St.C., Skipwith, P., 1964. Origin of the coastal flats, the sabhka of the Trucial coast, Persial Gulf. Nature 202, 759-761.

Eugster H.P., Hardie L.A., 1978. Saline lakes. In: Lerman A. (ed.), Lakes: Chemistry, Geology, Physics. Springer, New York, pp. 237-289.

Flower, G., Foster, I.D.L., 1992. Climatic implications of recent changes in lake level at Lac Azigza (Morocco). Bulletin de la Société Géologique de France 163 (1), 91-96.

Freytet, P., Verrechia, E.P., 2002. Lacustrine and palustrine carbonate petrography: an overview. Journal of Paleolimnology 27, 221-237.

García-Vera, M.A., San Román Saldaña, J., Blasco Herguedas, O., Coloma López, P., 2009. Hidrogeología de la Laguna de GalIocanta e implicaciones ambientales. In M.A. Casterad and C. Castañeda (eds.) La Laguna de Gallocanta: Medio natural, conservación y teledetección. Memorias de la Real Sociedad Española de Historia Natural 7, pp. 79-104. (In Spanish). Accessed on: http://digital.csic.es/bitstream/10261/61407/1/CasteradMA_LagunaGallocanta%28Lib%29_2009.pdf.

García-Vera, M.A., Martínez-Cob, A., 2004. Evolución del contenido de humedad y de la tasa de evaporación en humedales: aplicación a la Laguna de Gallocanta. 2004-PH-14-I, Zaragoza, Spain. (In Spanish) Available on: http://digital.csic.es/bitstream/10261/2976/1/InformeGallocanta2004-DEF.pdf.

Ghienne, J. F., Shcuster, M., Bernard, A., Duringer, P., Brunet, M., 2002. The Holocene giant Lake Chad revealed by digital elevation models. Quaternary International 87, 81-85.

Gómez, D., Monserrat, G., Ferrer, J., 1981. Aportación al estudio de la flora y vegetación en la cuenca endorreica de Gallocanta. In E. Aranzadi and J.J. Guiral (coord.), Estudio de la Biocenosis de la Laguna de Gallocanta y su cuenca, MOPU, Madrid, Spain, 982 pp. (In Spanish).

Gouramanis, C., Wilkins, D., De Deckker, P., 2010. 6000 years of environmental changes recorded in Blue Lake, South Australia, based on ostracod ecology and valve chemistry. Palaeogeography, Palaeoclimatology, Palaeoecology 297, 223-237.

Gracia, F.J., 1995. Shoreline forms and deposits in Gallocanta Lake (NE Spain). Geomorphology 11, 323-335.

Gracia, F.J., 2009. Geología y Geomorfología de la Laguna de Gallocanta. In M.A. Casterad and C. Castañeda (eds.) La Laguna de Gallocanta, Medio natural, conservación y teledetección. Memorias de la Real Sociedad Española de Historia Natural 7, pp. 59-76. (In Spanish). Accessed on:

http://digital.csic.es/bitstream/10261/61407/1/CasteradMA_LagunaGallocanta%28Lib%29_2009.pdf.

Gracia, F.J., 2014. Gallocanta Saline Lake, Iberian Chain. In: F. Gutiérrez and M. Gutiérrez (eds.), Landscapes and Landforms of Spain. World Geomorphological Landscapes, Springer Science+Business Media, Dordrecht, pp. 137-144.

Gracia, F.J., Gutiérrez, F., Gutiérrez, M., 2002. Origin and evolution of the Gallocanta polje (Iberian Range, NE Spain). Z. Geomorph. N.F. 46, 245-262.

Guilloré, P., 1985. Méthode de fabrication mécanique et en série des lames minces, 3th ed. (In French.) Institut National Agronomique, Paris-Grignon.

Gutiérrez, F., Gutiérrez, M., Gracia, F.J., McCalpin, J.P., Lucha, P., Guerrero, J., 2008. Plio-Quaternary extensional seismotectonics and drainage network development in the central sector of the Iberian Chain (NE Spain). Geomorphology 102, 21-42.

Hernández-Pacheco, F., Aranegui, P., 1926. La laguna de Gallocanta y la geología de sus alrededores. Bol. Real Soc. Española de Historia Natural 26, 419-429. (In Spanish) Accesed on http://bibdigital.rjb.csic.es/ing/Libro.php?Libro=1239

Hoffmann, N., Reicherter, K., Grützner, C., Hürtgen, J., Rudersdorf, A., Viehberg, F.A., Wessels, M., 2012. Quaternary coastline evolution of Lake Ohrid (Macedonia/Albania). Central European Journal of Geosciences 4 (1), 94-110.

Hunt, C.B., Washburn, A.L., 1966. Patterned ground. In USGS Prof. Papers 494-B, pp. 104-133.

Hurt, G.W., Vasilas L.M. (Eds.), 2006. Field indicators of hydric soils in the United States (Version 6.0), USDA, NRCS, Fort Worth, TX. http://soils.usda.gov/soil_use/hydric/field_ind.pdf.

Isla, F.I., Bassani, S., 1992. Evolución de costas y playas en lagos artificiales: Mari Menuco y Los Barreales, Neuquen, Argentina. In: VIII Congreso Latinoamericano de Geología, Salamanca, Vol. 4 Simps., pp. 404-408.

Komatsu, T., Watanabe, T., Hirakawa, K., 2010. A framework for Late Quaternary lake-level fluctuations in Lake Karakul, eastern Pamir, focusing on lake-glacier landform interaction. Geomorphology 119 (3-4), 198-211.

Jackson, J.A., 1997. Glossary of Geology, Fourth Edition, American Geological Institute, 769 pp.

Johnson, L.A., Haukos, D.A, Smith, L.M., McMurry, S.T., 2011. Loss of Playa Wetlands Caused by Reclassification and Remapping of Hydric Soils on the Southern High Plains. Wetlands 31, 483-492.

Leránoz, B., González, M., 2009. Historia, evolución y gestión de la Reserva Natural Dirigida de la Laguna de Gallocanta. Pp. 5-28. In M.A. Casterad and C. Castañeda (eds.) La Laguna de Gallocanta, Medio natural, conservación y teledetección. Memorias de la Real Sociedad Española de Historia Natural 7. (In Spanish). Accessed on: http://digital.csic.es/bitstream/10261/61407/1/CasteradMA_LagunaGallocanta%28Lib%29_2009.pdf.

Lindbo, D.L. Stolt, M.H. Vepraskas, M.J., 2010. Redoximorphic features. In Stoops, G., Marcelino, V., Mees, F. (eds.). Interpretation of Micromorphological Features of Soils and Regoliths. Their relevance for pedogenic studies and classifications. Elsevier, 752 pp.

Liso M., Ascaso, A., 1969. Introducción al estudio de la evapotranspiración y clasificación climática de la cuenca del Ebro. Anales de la Estación Experimental de

Aula Dei 10, 523 pp. (In Spanish). Accessed on: http://digital.csic.es/handle/10261/5565.

Luna, E., Latorre, B., Castañeda, C., 2014. Rainfall and the presence of water in Gallocanta Lake. Proceeding of the IX European Wetland Congress, Wetlands Biodiversity and Services: Tools for Socio-Ecological Development, Huesca, Spain, pp. 164.

Luzón, A., Pérez, A., Sánchez, J.A., Soria, A.R., & Mayayo, M.J, 2007a. Evolution from a freshwater to saline lake: a climatic or hydrogeological change? The case of Gallocanta Lake (northeast Spain). Hydrogeological Processes 21, 461-469.

Luzón, A., Pérez, A., Mayayo, M.J., Soria, A.R., Sánchez, M.F. & Roc, A.C. 2007b. Holocene environmental changes in the Gallocanta lacustrine basin, Iberian Range, NE Spain. The Holocene 17, 649-663.

Machette, M.N., 1985. Calcic soils of the southwestern United States. In D.L. Weide (ed.) Soils and Quaternary geomorphology of the southwestern United States. Geological Society of America Special Paper 203.

Martínez-Cob, A., Zapata, N., Sánchez, I., 2010. Viento y riego. La variabilidad del viento en Aragón y su influencia en el riego por aspersión. Institución Fernando El Católico. Zaragoza, Spain, 200 pp. (In Spanish)

Mason, I.M., Guzkowska, M.A.J., Rapley, C.G., Street-Perrott, F.A., 1994. The response of lake levels and areas to climatic change. Climatic Change 27(2), 161-197.

Merlín-Uribe, Y., Contreras-Hernández, A., Astier-Calderón, M., Jensend, O.P., Zaragoza, R., Zambrano, L., 2011. Urban expansion into a protected natural area in Mexico City: alternative management scenarios. Journal of Environmental Planning and Management 56(3), 398-411.

Neal, J.T., 1972. Playa surfaces features as indicators of environment. Playa-lake Symp. Proc., ICSCALS Publ. 4. Texas Tech University. Lubbock, Texas, pp. 107-132.

Ocakoglu, F., Kir, O., Yilmaz, I.O., Acikalin, S.; Erayik, C., Tunoglu, C., Leroy, S.A.G., 2013. Early to Mid-Holocene lake level and temperature records from the terraces of Lake Sünnet in NW Turkey. Palaeogeography, Palaeoclimatology, Palaeoecology 369, 175-184.

Otero, X.L., Macías, F., 2001. Caracterización y clasificación de suelos de las Marismas de la Ría de Ortigueira en relación con su posición fisiográfica y vegetación (Galicia-NO de la Península ibérica). Edafología 8(3), 37-61.

Pérez, E., 2014. Recordando Gallocanta, 1972-1984. Boletín de la Real Sociedad Española de Historia Natural Sección Biológica 108, http://historia.bio.ucm.es/rsehn/index.php?d=publicaciones&num=34&w=242&ft=1.

Pérez, A., Luzón, A., Roc, A.C., Soria, A.R., Mayayo, M-J-, Sánchez, J.A., 2002. Sedimentary facies distribution and genesis of a recent carbonate-rich saline lake: Gallocanta Lake, Iberian Chain, NE Spain. Sedimentary Geology 148, 185-202.

Platt, N.H., 1989. Lacustrine carbonates and pedogenesis: sedimentology and origin of palustrine deposits from the Early Cretaceous Rupelo Formation, W Cameros Basin, N Spain. Sedimentology 36, 665-684.

Plotnikov, I.S., Aladin, N.V., 2011. An overview of hybrid marine and lacustrine seas and saline lakes of the world. Lakes & Reservoirs: Research and Management 16, 97-108.

Ramsar Convention Secretariat, 2010. Ramsar Handbooks for the Wise Use of Wetlands, 4th ed., vol 1. Ramsar Convention Secretariat, Gland (Switzerland). 56 pp.

Richardson, J.L., Vepraskas, M.J., 2001. Wetland soils: Genesis, Hydrology, Landscapes and Classification. CRC Press, Boca Raton, Florida, 417 pp.

Rodó, X. Giralt, S., Burjachs, F., Comín, F., Tenorio, R.G., Julià, R., 2002. High-resolution saline lake sediments as enhanced tools for relating proxy paleolake records to recent climatic data series. Sedimentary Geology 148, 203-220.

Ruhe, R.V., 1959. Stone lines in soils. Soil Science 84, 223-231.

Schoeneberger, P.J., D.A. Wysocki, E.C. Benham, and Soil Survey Staff, 2012. Field book for describing and sampling soils, Version 3.0. Natural Resources Conservation Service, National Soil Survey Center, Lincoln, NE.

Schütt, B., 1998. Reconstruction of Holocene paleoenvironments in the endorheic basin of Laguna de Gallocanta, Central Spain by investigation of mineralogical and geochemical characters from lacustrine sediments. Journal of Paleolimnology 20, 217-234.

Soil Survey Staff, 2014. Keys to Soil Taxonomy, 12th ed. USDA - Natural Resources Conservation Service. Washington, DC, 360 pp.

Splinter, D.K., Dahmas, D.E., may, D.W., 2005. Soils and Geomorphology of the Lower Little Cedar River Valley, Northeast Iowa, Physical Geography 26(1), 52-68.

Stoops, G., 2003. Guidelines for Analysis and Description of Soil and Regolith Thin Sections. Soil. Science Society of America, Inc. Madison, Wisconsin, USA. X pp. 184.

Taubner, H., Roth, B., Tippkotter, R., 2009. Determination of soil texture: comparison of the sedimentation method and the laser-diffraction analysis. Journal of Plant Nutrition and Soil Sciences 172, 161-171.

United States Salinity Laboratory Staff, 1954. Diagnosis and Improvement of Saline and Alkali Soils. Agriculture Handbook 60. USDA, Washington, D.C.

Vinogradov, B.V., 1955. Macropolygonal structure of clay plains. Doklady Akademi Nauk SSSR, 104: 118-120. Translated into English in J.T. Neal (ed.): Playas and dried lakes. Benchmark Papers in Geology 20, Dowden, Hutchinson & Ross, Stroudsburg, pp. 323-326.

Vepraskas, M.J., 1994. Redoximorphic features for identifying aquic conditions. Tech. Bull. 301, NC Agric. Res. Serv., Raleigh. Revised and reprinted 1994.

List of Figures

Figure 1. Geological map (after García-Vera et al., 2009), the main streams, and weather stations within the study area at Gallocanta Lake.

Figure 2. Water depth of Gallocanta Lake from 1974 to 2002 (García-Vera et al., 2009).

Figure 3. Location of the soil profile sites in two margins in the central section of Gallocanta Lake. Orthophotographs were taken in 2006-2007. The main arroyos are indicated in blue. Black rectangles indicate the location of the areas shown in Figs. 4 and 6.

Figure 4. Geomorphological map of a section of the NE shoreline within the central section of Gallocanta Lake (slightly modified from Castañeda et al., 2013). The six soil sampling sites are indicated, GA23 to GA28.

Figure 5. The NE shoreline of Gallocanta Lake in summer 2013. A: Alluvial fans that extend from the base of the mountain, the vegetated lake margin, and the dry lake. B: sand barrier covered with pioneering halophytes; C: The lake floor and a vegetated marginal wetland with *Juncus*. Geographical locations are indicated in Fig. 4.

Figure 6. Geomorphological map of the SW shoreline of the central section of Galllocanta Lake (modified from Castañeda et al., 2013). Five soil sampling sites are indicated (GA19 to GA22 and GA29).

Figure 7. The SW shoreline of Gallocanta Lake in summer 2013. A: Near the mouth of Los Pozuelos arroyo, where it intersects a littoral sand bar; several small gullies erode the sands and form small alluvial fans on the dry arroyo thalweg. B: Sublittoral bar, emerged during a dry period, with tumbleweeds (*Salsola kali*) trapped on the silty surface.

Figure 8. Soil salinity (ECe) in the 11 pedons at Gallocanta Lake, expressed as the values from 25-cm-thick synthetic soil layers.

Figure 9. Macromorphological features of the soil profiles at the NW and SW margins of the central section of Gallocanta Lake.

Figure 10. Micromorphological features of palustrine horizons at Gallocanta Lake. A: Lenticular gypsum accumulation and peloidal microstructure (GA19, Ag). B: Blocky microstructure (GA20, 4Cg4). C: Pendant with sequential aggradation and dark rims (GA22 Bwk); D: Calcite-rich groundmass with crystallitic b-fabric and carbonate coatings (GA19, 2Cg2). E: Carbonate crystals (GA20, 2Cg2). F: Charophyte oogonia (GA19, Ag); G: Ostracod shell remains in paleovalley soils (GA22, Bwk). H: Fe-Mn impregnative hypocoatings (GA19, Ag).

Figure 11. Soil composition along the soil transects at the NW and SW margins of Gallocanta Lake. The topographic profile and the main geomorphological features are indicated.

Figure 12. (A) Composite aerial contact prints of the central section of Gallocanta Lake, taken in September 1975 (from Pérez, 2014), and (B) ortophotograph taken in September 2006.

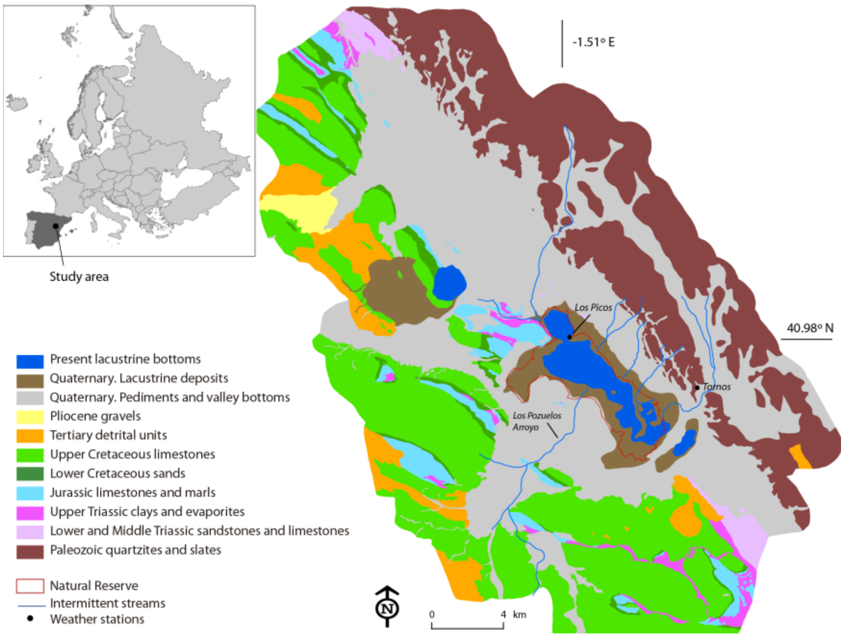

Figure 1

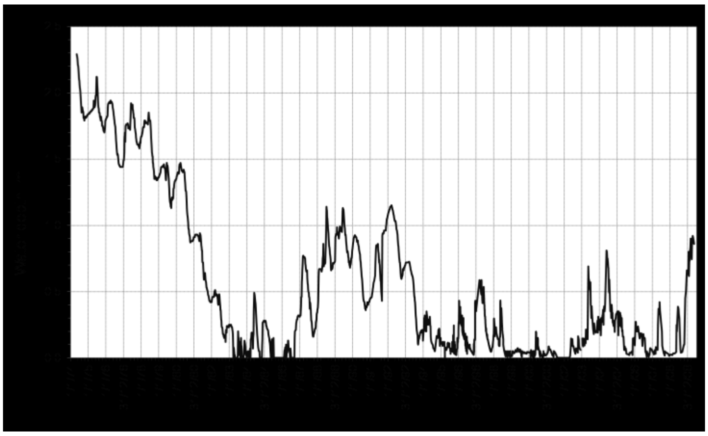

Figure 2

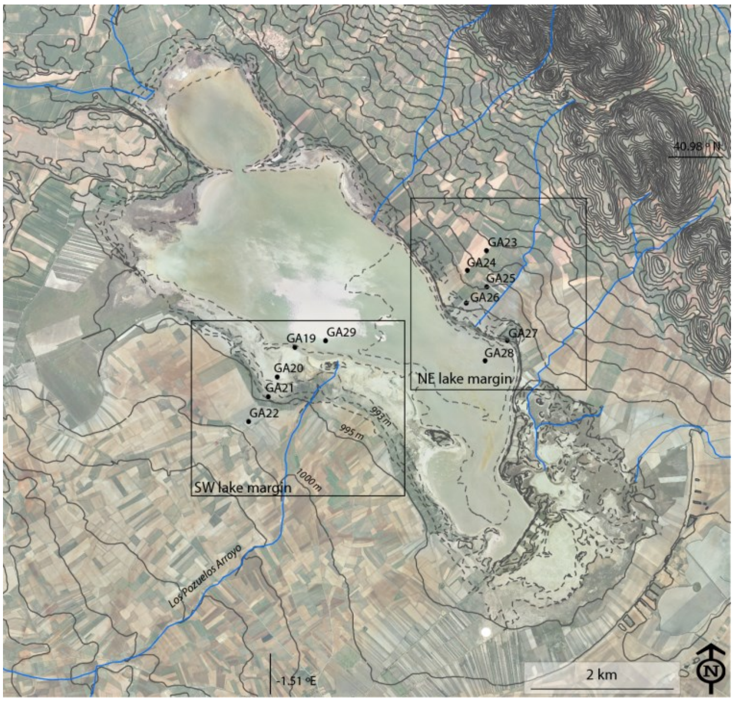

Figure 3

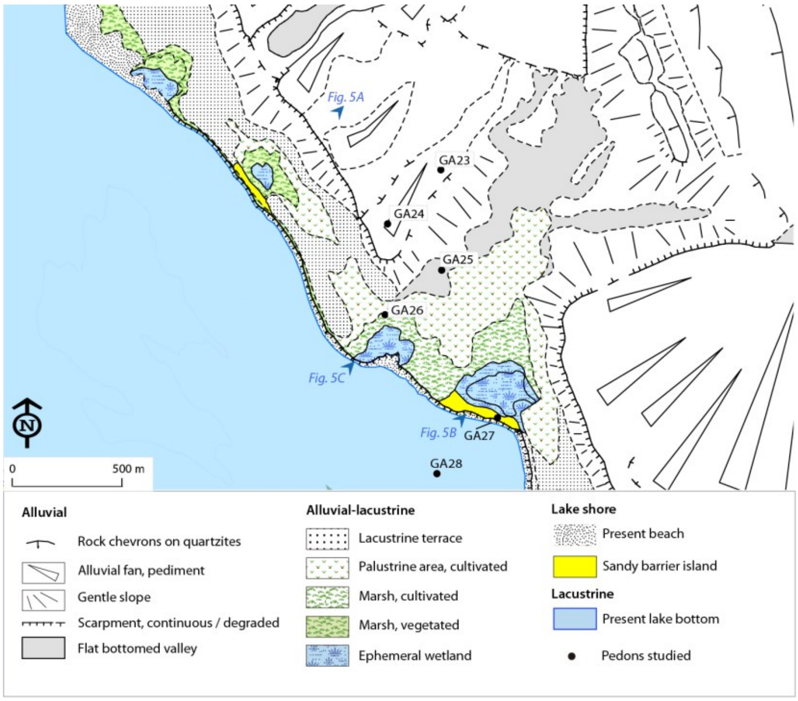

Figure 4

Figure 5

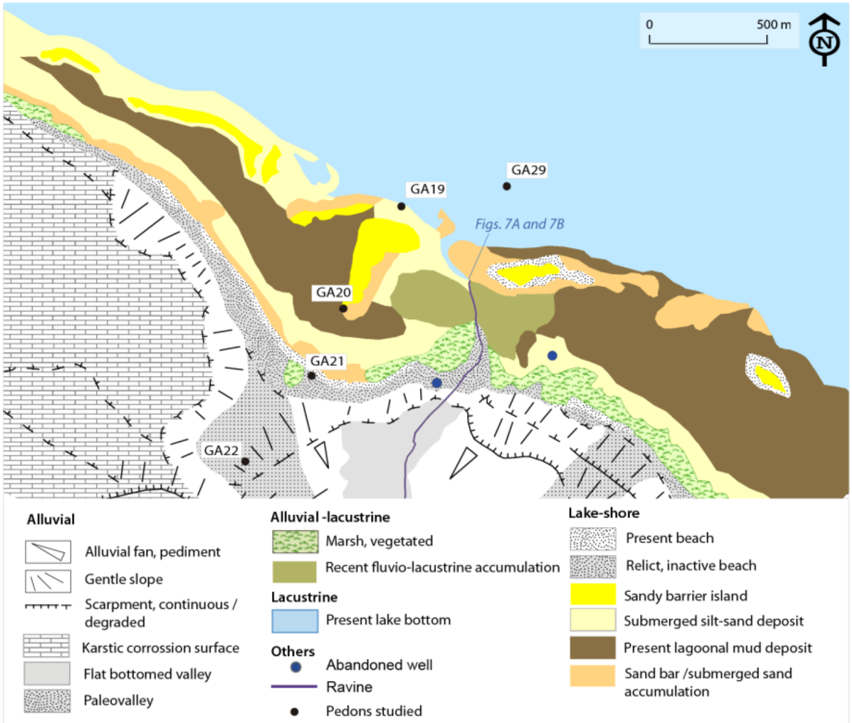

Figure 6

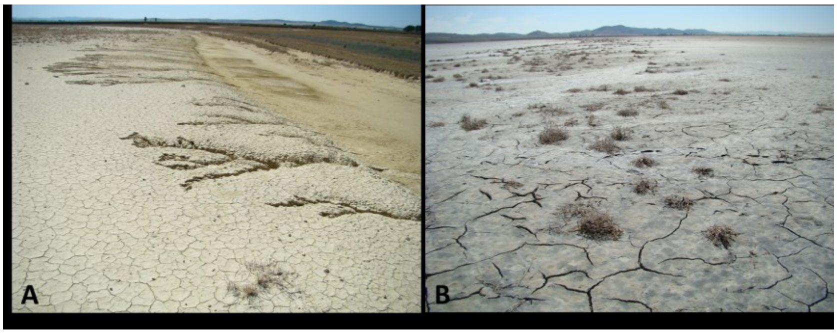

Figure 7

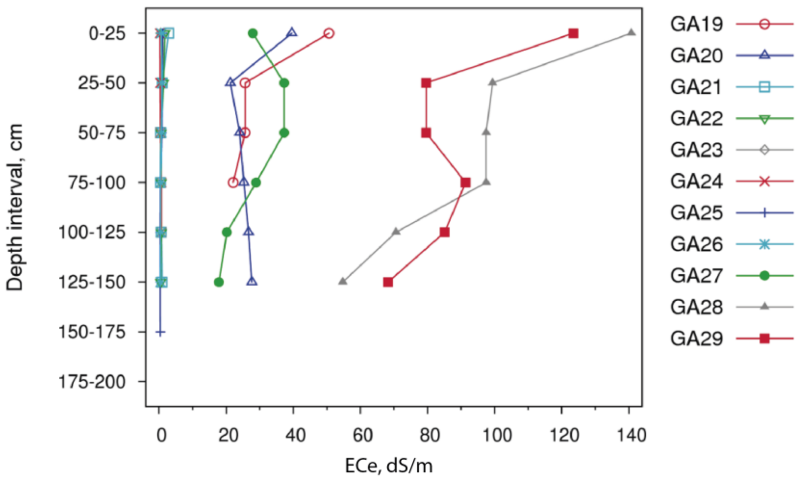

Figure 8

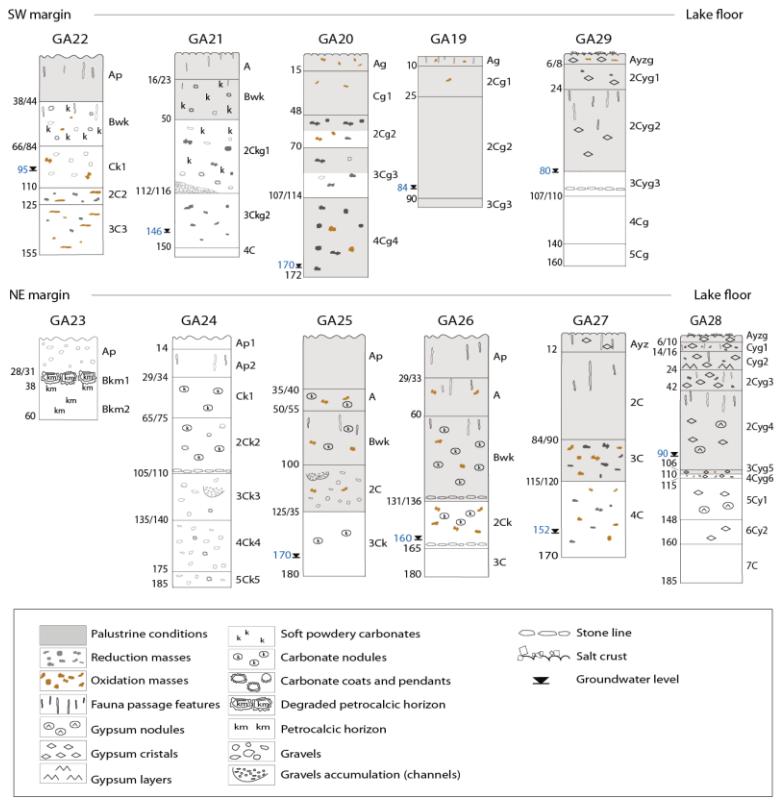

Figure 9

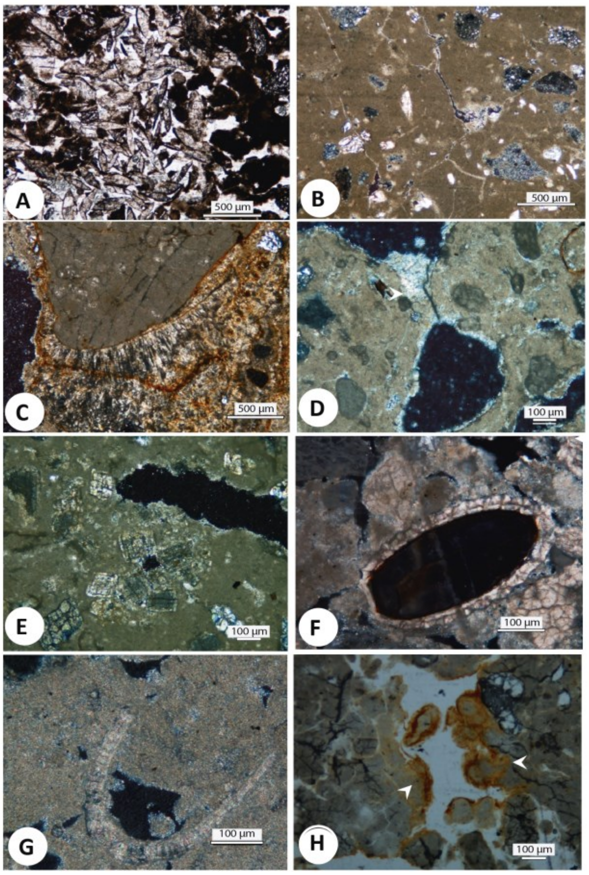

Figure 10

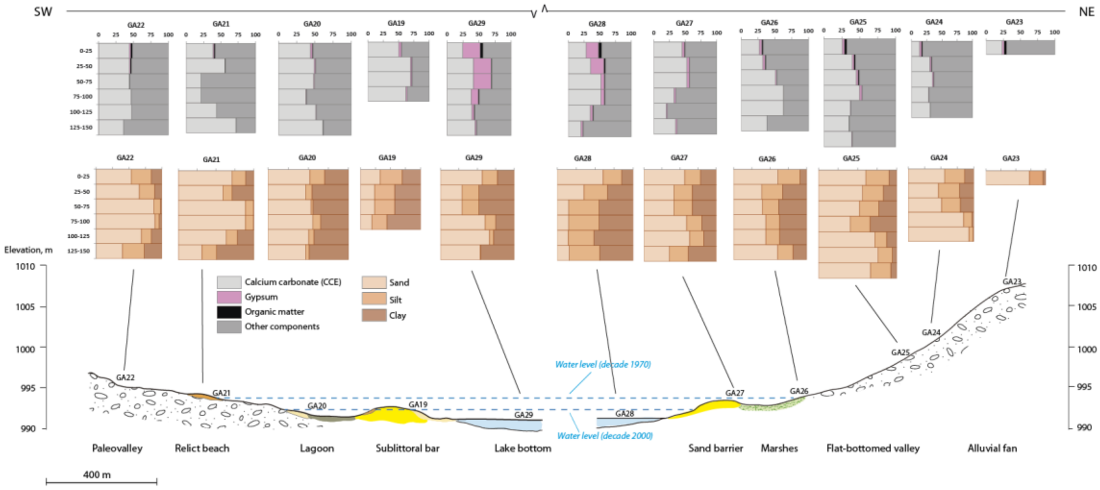

Figure 11

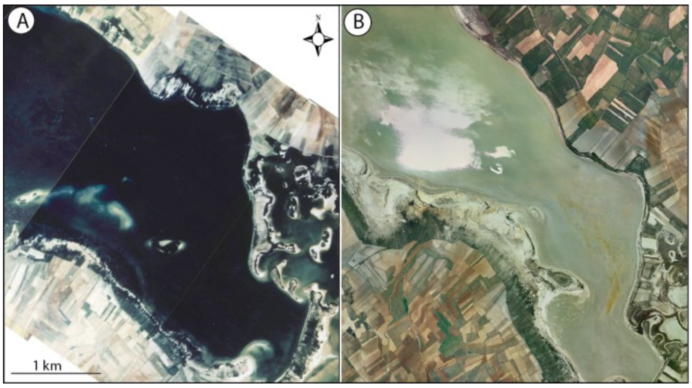

Figure 12